THE JOURNAL OF BIOLOGICAL CHEMISTRY VOL. 282, NO. 49, pp. 35712–35721, December 7, 2007

The ADAM10 Prodomain Is a Specific Inhibitor of ADAM10 Proteolytic Activity and Inhibits Cellular Shedding Events*

Received for publication, April 17, 2007, and in revised form, September 20, 2007 Published, JBC Papers in Press, September 25, 2007, DOI 10.1074/jbc.M703231200

Marcia L. Moss[‡1], Martha Bomar[§], Qian Liu[§], Harvey Sage[§], Peter Dempsey[¶], Patricia M. Lenhart[¶], Patricia A. Gillispie[¶], Alexander Stoeck[¶], Dirk Wildeboer[‖], Jörg W. Bartsch[‖], Ralf Palmisano[**], and Pei Zhou[§2]

From [‡]BioZyme Incorporated, Apex, North Carolina 27523, the [§]Department of Biochemistry, Duke University Medical Center, Durham, North Carolina 27710, the [¶]Departments of Pediatrics and Molecular and Integrative Physiology, University of Michigan, Ann Arbor, Michigan 48109, the [‖]Department of Biochemistry, King's College London, London SE1 9NH, United Kingdom, and the [**]Faculty of Biology, University of Bielefeld, 33615 Bielefeld, Germany

ADAM10 is a disintegrin metalloproteinase that processes amyloid precursor protein and ErbB ligands and is involved in the shedding of many type I and type II single membrane-spanning proteins. Like tumor necrosis factor-α-converting enzyme (TACE or ADAM17), ADAM10 is expressed as a zymogen, and removal of the prodomain results in its activation. Here we report that the recombinant mouse ADAM10 prodomain, purified from *Escherichia coli*, is a potent competitive inhibitor of the human ADAM10 catalytic/disintegrin domain, with a K_i of 48 nM. Moreover, the mouse ADAM10 prodomain is a selective inhibitor as it only weakly inhibits other ADAM family proteinases in the micromolar range and does not inhibit members of the matrix metalloproteinase family under similar conditions. Mouse prodomains of TACE and ADAM8 do not inhibit their respective enzymes, indicating that ADAM10 inhibition by its prodomain is unique. In cell-based assays we show that the ADAM10 prodomain inhibits betacellulin shedding, demonstrating that it could be of potential use as a therapeutic agent to treat cancer.

Members of the a disintegrin and metalloproteinase (ADAM)[3] family of proteolytic enzymes play important roles in many cellular signaling processes. They function as sheddases by cleaving type I and type II integral single membrane proteins to generate soluble mature forms (1–3). ADAM family members typically contain several domains as follows: a prodomain, a catalytic and cysteine-rich disintegrin domain, a transmembrane region, and a cytoplasmic tail (4). Prodomains are required for successful production of ADAM family members. For example, TACE and ADAM12 require their prodomains for efficient transport, folding, and expression (5–7). Similarly, the prodomain of ADAM10 acts as a molecular chaperone to allow the expression of catalytically active ADAM10 (8).

ADAM family members are expressed as zymogens with the prodomains maintaining the enzymes in a latent state. Isolated prodomains have been shown to inhibit the proteolytic activity of ADAM family proteins *in vitro* (9). However, not all prodomains are good inhibitors. For example, although the prodomain of TACE suppresses the activity of its catalytic domain with a K_i of 50 nM (9), it is only a high micromolar inhibitor against the TACE construct, including both the catalytic and disintegrin domains. Because the catalytic and disintegrin domains are both retained in membrane-bound TACE, the prodomain, once removed, most likely does not negatively affect TACE activity *in vivo*.

ADAM family members are zinc metalloproteinases, and their catalytic activity depends on the activation of the zinc-bound water and subsequent nucleophilic attack on the amide backbone of a protein substrate. The inhibitory mechanism, in which the prodomain interferes with metalloproteinase activity by replacing the zinc-bound water with a cysteine residue, is known as "the cysteine switch" and was originally described for members of the matrix metalloproteinase (MMP) family (10). For ADAM12, the cysteine is required for inhibition of the catalytic activity when an α_2-macroglobulin assay is used to assess catalytic activity (7). However, mutation of the corresponding cysteine to alanine in the putative cysteine switch region of TACE does not diminish the inhibitory properties of the prodomain, suggesting that the cysteine switch hypothesis is invalid for this family member (9).

Biologically important substrates of ADAM10 include epidermal growth factor (EGF) (11), betacellulin (11), Notch (12), and amyloid precursor protein (APP) (13). Consequently, misregulation of ADAM10 catalytic activity is implicated in Alzheimer disease and carcinogenesis. For example, α-secretases such as ADAM10 and other metalloproteinases can carry out the first cleavage reaction of APP (14). Disruption of ADAM10 activity has been shown to decrease the level of sol-

* This work was supported by the Whitehead Institute, King's College London (to J. W. B.), by National Institutes of Health T32 Training Grant, by National Institutes of Health Grants DK59778 and DK63363, and by a Crohns and Colitis Foundation of America grant (to P. J. D.). The costs of publication of this article were defrayed in part by the payment of page charges. This article must therefore be hereby marked "*advertisement*" in accordance with 18 U.S.C. Section 1734 solely to indicate this fact.

[1] To whom correspondence may be addressed: BioZyme Inc., 1513 Old White Oak Church Rd., Apex, NC 27523. Tel.: 919-362-1339; Fax: 919-362-1339; E-mail: mmoss@biozyme-inc.com.

[2] To whom correspondence may be addressed: Dept. of Biochemistry, Duke University Medical Center, Rm. 242, Nanaline Bldg., Research Dr., Durham, NC 27710. Tel.: 919-668-6409; Fax: 919-684-8885; E-mail: peizhou@biochem.duke.edu.

[3] The abbreviations used are: ADAM, a disintegrin and metalloproteinase; aa, amino acid; APP, amyloid precursor protein; AR, amphiregulin; BTC, betacellulin; dabcyl, 4-(4-dimethylaminophenylazo)benzoyl; Me_2SO, dimethyl sulfoxide; EGF, epidermal growth factor; EGFR, EGF receptor; IFNγ, interferon-γ; IMPE, immortalized pancreatic epithelial cells; Pro, prodomain; TACE, tumor necrosis factor-α converting enzyme; Ni-NTA, nickel-nitrilotriacetic acid; CHAPS, 3-[(3-cholamidopropyl)dimethylammonio]-1-propanesulfonic acid; DMEM, Dulbecco's modified Eagle's medium; MMP, matrix metalloproteinase.

uble nonamyloidogenic APP both *in vivo* and in cell-based assays (15), suggesting that maintaining ADAM10 activity may play a protective role in Alzheimer disease for processing of APP via the α-secretase pathway. In contrast, excess ADAM10 activity may promote cell growth in cancer proliferation assays because of enhanced production of soluble mature forms of several ErbB ligands such as betacellulin (BTC) and EGF (2, 11). Blocking EGF receptor (EGFR) signaling in cancer by EGFR kinase inhibitors or antibodies that neutralize EGFR are current ways to regulate tumor growth (16, 17). A novel way to repress EGFR signaling could be through inhibition of ADAM10-dependent substrate processing of soluble ErbB ligands because ADAM10 is a known sheddase of BTC and EGF (11), and soluble forms activate EGFR by causing receptor dimerization (2). As a result, specific and potent inhibitors of ADAM10 could be used to suppress tumor progression *in vivo*.

We have undertaken studies to express, purify, and test a prodomain construct based on the mouse ADAM10. A number of parameters were varied to obtain high expression levels of soluble protein. To study the cysteine switch mechanism, we introduced a mutation by exchanging the cysteine to serine in the ADAM10 prodomain. We show that the C173S mutation does not impair the inhibitory potency of the prodomain against ADAM10. Measurements of the inhibition of ADAM10 prodomains against ADAM8–10 and -17 and MMPs demonstrate that the wild type and mutant prodomain are selective inhibitors against ADAM10. ADAM10 prodomain inhibits betacellulin shedding in cell-based assays *in vitro*, and thus may become an attractive approach for the treatment of various cancers.

EXPERIMENTAL PROCEDURES

Materials

Human ADAM10, ADAM9, and TACE protease containing the catalytic/disintegrin domains were obtained from R & D Systems (Minneapolis, MN). The following enzymes were generously donated to us: TACE catalytic domain from Marcos Milla, University of Pennsylvania; MMP-1 and -3 from Hideaki Nagase, Imperial College London; MMP-2 and -9 from William Stetler-Stevenson, NCI, National Institutes of Health; MMP-13 and -14 from Gillian Murphy, Cambridge University. All fluorescent-labeled peptides were either purchased from SynPep Corp. (Dublin, CA) or obtained from BioZyme Inc. (Apex, NC). Dinitrophenyl-labeled peptides were purchased from the University of North Carolina, Chapel Hill, peptide synthesis laboratory. All oligonucleotides for PCR and directed mutagenesis were ordered from IDT DNA (Coralville, IA).

Methods

Cloning of ADAM Family cDNA—A DNA fragment containing ADAM10 prodomain (residues 23–213) was cloned into the pRSET vector (Invitrogen) between BamHI and EcoRI sites to produce an N-terminal His-tagged protein, or cloned into a modified pET30a vector (EMD Biosciences, Madison, WI) between NdeI and BamHI sites as a C-terminal His-tagged protein. The modified pET30a vector encodes His_6 between BamHI and EcoRI sites to produce a protein with a C-terminal His tag. DNA primers were as follows: N-terminal and C-terminal His tag 23–213, 5′ primer, GGA GCC GGA TCC AAT CCT TTA AAT AAA TAT ATT, and 3′ primer, GGA GCC GAA TTC TTA GCG TTT TTT CCT CAG GAG CTC; N-terminal and C-terminal His tag 23–213, 5′ primer, GGA GCC CAT ATG AAT CCT TTA AAT AAA TAT ATT, and 3′ primer, GGA GCC GGA TCC TTT TTT CCT CAG GAG CTC AGG; and C-terminal His tag 23–181, GGA GCC CAT ATG AAT CCT TTA AAT AAA TAT ATT, and 3′ primer, GGA GCC GGA TCC CCT TTC AAA AAC GGA GTG ATC. The wild type 23–213 C-terminal His-tagged ADAM10 prodomain was used as a template to mutate cysteine 173 to serine. The DNA primers for site-directed mutagenesis were 5′ primer, AAA TAC GGC CCA CAG GGC GGC TCT GCA GAT CAC TCC GTT TTT GAA, and 3′ primer TTC AAA AAC GGA GTG ATC TG AGA GCC CC CTG GG GCC GTA TTT.

For prodomains of TACE 18–214 and ADAM8 18–186, mouse full-length cDNAs were used as templates to prepare fragments that were subcloned into the same vector as described for ADAM10. For truncated prodomains 23–176 and 23–181, the 23–213 construct was used as a template, and the fragments were subcloned into the same C-terminal His vector as described above. For prodomain 18–176, the full-length ADAM10 was used as a template, and fragments were subcloned into either N- or C-terminal His constructs.

Expression and Purification—The appropriate constructs were transformed into *Escherichia coli* BL21(DE3)STAR cells. For a typical sample preparation, bacteria were grown in 1 liter of Luria Broth at 37 °C until the A_{600} reached 0.4. The culture was incubated at 20 °C for 30 min before adding isopropyl β-D-thiogalactopyranoside (1 mM) to induce protein expression. Cells were harvested after 16 h by spinning at 4 °C for 30 min at 4000 rpm in a Sorvall JA 10 rotor. The supernatant was removed, and pellets were either stored at −20 °C or used directly.

Cell pellets were lysed by French press at 1100 p.s.i. in 25 ml of buffer containing 50 mM phosphate, pH 8.0, 10 mM imidazole, and 300 mM NaCl at 4 °C or lysed with the same buffer with cell lytic from Sigma (3 ml of a 10× concentrated solution), benzonase (1500 units), and lysozyme (0.2 mg/ml). For the wild type constructs, 0.1% β-mercaptoethanol was added to each buffer to minimize oxidation of cysteine. Lysed bacteria were spun at 21,500 rpm in a Beckman JA 25.50 rotor for 30–60 min. The cleared supernatant was applied to a 15-ml Ni^{2+}-NTA column pre-equilibrated with lysis buffer. After two 30-ml washes with a solution containing 50 mM phosphate, pH 8.0, 20 mM imidazole, and 300 mM NaCl, the protein was eluted with a solution containing 50 mM phosphate, pH 8.0, 250 mM imidazole, and 300 mM NaCl. The eluted protein was concentrated to less than 2 ml using an Amicon ultrafiltration device (molecular mass cutoff of 10 kDa) from Millipore (Billerica, MA) and further purified with a Superdex-75 column (150 ml) on an Akta FPLC system at a flow rate of 1 ml/min. FPLC buffers contained 25 mM phosphate, pH 7.0, 100 mM NaCl, or 25 mM Tris, pH 8.0, 100 mM NaCl. Fractions containing protein were concentrated and passed through an Endotrap column from Profos to remove any residual endotoxin and then stored as glycerol stocks at −80 °C. Monomer concentration was determined

based on a calculated extinction coefficient at A_{280} for the prodomain using the program ExPASy.

Ultracentrifugation—The molecular weight of ADAM10 prodomain in 25 mM phosphate, pH 7.0, 150 mM KCl was estimated by sedimentation equilibrium at 15,000 and 20,000 rpm and at 25 °C on a Beckman model XL-A analytical Ultracentrifuge. The $\bar{\nu}$ of the protein and ρ of the solvent were estimated to be 0.7216 and 1.005, respectively, by the SEDNTRP program. The protein was examined at several concentrations (0.45, 0.9, and 1.8 mg/ml) and was monitored by the absorbance at 286 nm. The nonlinear least square curve was generated by the IDEAL1 program (Beckman).

Circular Dichroism Spectroscopy—A 30 μM sample of the 23–213 ADAM10 construct in a buffer containing 25 mM phosphate and 50 mM NaCl, pH 8.0, was used to obtain a CD spectrum on an Aviv 202 CD spectrometer. A wavelength scan from 200 to 300 nm was collected in a 1-mm quartz cuvette at 25 °C. Scans were obtained in 1-nm increments with a signal averaging time of 5 s. Background noises from the buffer were subtracted from the raw CD signal.

Inhibition Assays with TACE and ADAM10—Activity of TACE catalytic/disintegrin, TACE catalytic, or ADAM10 catalytic/disintegrin constructs was monitored at 3-min intervals using the fluorescent substrate, dabcyl-LAQAHomoPheRSC(fluorescein)-NH_2 (18) with excitation at 485 nm and emission at 530 nm. The substrate was diluted from a 10 mM stock in Me_2SO to 10 μM in assay buffer containing 20 mM Tris, pH 8.0, and 6×10^{-4}% Brij-35. Reactions were run in a 96-well black-coated plate with either ADAM10 prodomain (10 nM to 1.0 μM) alone or with enzyme. Concentrations of enzyme ranged from 0.5 to 2.0 nM for TACE and from 5 to 15 nM for ADAM10. For assays with TACE and ADAM8 prodomain, the range of concentrations varied from 1 to 4.7 μM.

Inhibition Assays with MMPs—The fluorescent substrate dabcyl-GPLGMRGC(fluorescein)-NH_2 (19) in assay buffer (10 μM) containing 50 mM Tris, pH 7.5, 150 mM NaCl, 2 mM $CaCl_2$, 5 μM $ZnSO_4$, and 0.01% Brij-35 was used to monitor enzyme activities. MMP-1, -2, -3, -9, -13, and -14 (0.1–20 nM) were incubated with substrate in the absence or presence of prodomain (3–30 μM). Fluorescence intensities were measured every 3–5 min at an emission wavelength of 530 nm (excitation 485 nm).

Inhibition Assays with ADAM9—The fluorescent substrate, dabcyl-PchaGC(Me)HAK(5-carboxyfluorescein)-NH_2 (10 μM) (18), in a buffer containing 25 mM Tris, pH 8.0, 6×10^{-4}% Brij-35, was used to measure human ADAM9 catalytic/disintegrin domain activity. The ADAM9 was provided as a 0.1 μg/μl stock solution, from which 3 μl was added to start the reaction in the absence or presence of ADAM10 prodomain (78–5000 nM). Fluorescence intensities were measured every 10–20 min at excitation and emission wavelengths of 485 and 530 nm, respectively.

Inhibition Assays with ADAM8—The ADAM 8 catalytic domain was expressed and purified from *E. coli* as described (20). A substrate based on the L-selectin cleavage site, dinitrophenylalanyl-INorleuQKLDKSFSMIKE-NH_2, was used to monitor enzyme activity with a fluorescamine assay. From a concentrated 50 mM solution in Me_2SO, the substrate was diluted 1:500 in 25 mM HEPES, pH 8.0, 6×10^{-4}% Brij-35. To 100 μl of diluted substrate was added either 5 μl of buffer (Tris, pH 8.0, 150 mM KCl) or 5 μl of ADAM10 prodomain (1–10 μM). Zero time points were taken by diluting 12.5 μl of the reaction mixture into 100 μl of fluorescamine buffer (50 mM HEPES, pH 8.0, 0.2 M NaCl, 0.01 M $CaCl_2$, 0.01% Brij-35) in a 96-well black-coated plate. Before measuring fluorescence, 3 μl of a 1% solution of fluorescamine in Me_2SO was added to each well. The plate was allowed to incubate for 10 min in the dark before measuring fluorescence (excitation wavelength at 390 nm and emission wavelength at 485 nm). For assays with TACE and ADAM8 prodomains, dabcyl/5-carboxyfluorescein fluorescent substrates were used to monitor activity at concentrations of prodomains ranging from 1 to 4.7 μM (18).

Calculation of Inhibition Constants—The amount of activity was calculated by subtracting the prodomain control from the prodomain with enzyme. All inhibition assays were performed at room temperature and the data fit to Equation 1 using Sigma Plot software,

$$I_f = \frac{I}{(I + K_i)} \qquad \text{(Eq. 1)}$$

I_f is fractional inhibition; I is the inhibitor concentration, and K_i is the inhibition constant.

Mechanism of Inhibition—ADAM10 was diluted 1:100 in buffer 25 mM Tris, pH 8, 6×10^{-4}% Brij-35, and 10 μl was then added to 88 μl of substrate (20–100 μM), dabcyl-LAQAHomoPheRS-C(fluorescein)-NH_2 (21) with excitation at 485 nm and emission at 530 nm. Prodomain, 2 μl, in 25 mM Tris, pH 8, 100 mM NaCl, 10% glycerol, 0.1% mercaptoethanol, and 50 μM $CaCl_2$ was added to the substrate before addition of enzyme. The final concentration of prodomain ranged from 17 to 170 nM. The fluorescence *versus* time was plotted, and slopes were taken from straight line fits of initial velocities. The reciprocal of the velocities was plotted *versus* the reciprocal of substrate squared because the normal Lineweaver Burke plot gave curved lines. The initial velocities *versus* substrate concentrations were fit as a family of curves to several allosteric models. The data fit best to a pure competitive model as described in Equation 2 (2) where binding of inhibitor prevents substrate from binding to both sites.

$$v = V \times \left(\frac{S}{K_s} + \frac{S^2}{K_s^2}\right) \Big/ \left(1 + \frac{2S}{K_s} + \frac{S^2}{K_s^2} + \frac{I}{K_i}\right) \qquad \text{(Eq. 2)}$$

In this equation, v is the velocity obtained from the fluorescence units *versus* time plot; V is the maximum velocity; S is the substrate concentration; I is the inhibitor concentration; K_s is the dissociation constant for substrate binding to enzyme; and K_i is the inhibition constant.

Ligand Shedding Assays—The conditionally immortalized pancreatic epithelial (IMPE) cell line (22) was stably transduced with the retrovirus pBM BTC-HA IRES Puro expressing human BTC cDNA with a C-terminal HA tag as described previously (23) or with pBM AR IRES Puro expressing human amphiregulin. Cells were routinely cultured at 33 °C in Dulbecco's modified Eagle's medium (DMEM) plus 5% bovine growth serum/penicillin/streptomycin/nonessential amino acids

and 5 units/ml IFNγ and 2 μg/ml puromycin. For BTC shedding assay, cells were seeded at 5×10^4 cells/well in 24-well plates and grown for 48 h to confluence at 33 °C in medium containing IFNγ and then for an additional 36 h at 37 °C in medium lacking IFNγ and puromycin.

For all shedding assays, cells were pretreated for 30 min at 37 °C with serum-free DMEM containing vehicle control (Me_2SO), varying quantities of GI254023X and GW280264X or different concentrations of either buffer control or ADAM10 prodomain. For analysis of constitutive shedding, media were then replaced with fresh serum-free media using the same experimental treatments and incubated for 4 h at 37 °C. To evaluate stimulated ligand shedding, media were then replaced with fresh media using the same experimental treatments containing 2 μM A23187 and incubated for 1 h at 37 °C.

Conditioned media (CM) and cell lysates were then harvested as described previously (23). Specific human BTC and human AR sandwich enzyme-linked immunosorbent assays (R & D Systems) were used to quantify BTC and AR levels, respectively, in CM and cell lysates according to the manufacturer's instructions. The recombinant human BTC and human AR (R & D Systems) were used as standards for their respective assays. All experiments were repeated at least three times with similar results, and a representative figure is presented. Values for each experiment are expressed as the means ± S.E. of quadruplicate determinations.

Antibodies—Polyclonal antibodies were raised against the prodomain peptide (YGNPLNKYIRHYEGL) and a peptide representing the cytoplasmic domain (QPIQQPPRQRPRESY) of ADAM10. Antibodies were further purified by protein A-Sepharose chromatography.

Cell Culture—COS1 cells were grown in DMEM (Invitrogen) containing 10% fetal calf serum and 1% glutamine. Transient transfections were performed with the DEAE-dextran method (24).

Immunofluorescence—COS1 cells were grown on coverslips and transfected with the construct encoding full-length mouse ADAM10. 48 h after transfection, cells were fixed with 3.7% paraformaldehyde. To detect ADAM10, the polyclonal antibodies a-A10cyt (1:200) and a-A10pro (1:200) were used as primary antibodies. As secondary antibodies, we used either goat anti-rabbit-Cy3 (1:500, Sigma) or goat anti-rabbit-Alexa488 (1:500, Dako). Double stainings were performed sequentially. Between individual stainings, samples were incubated with anti-rabbit IgG (1:50, Sigma) to saturate excess binding sites. Images were acquired by confocal laser scanning microscopy (TCS SP2, Leica, Germany).

Immunoprecipitation Experiments—5×10^5 COS1 cells were transfected with 5 μg of DNA using the DEAE-dextran method (20). 48 h after transfection, cells were lysed in Co-IP buffer (50 mM Tris-Cl, pH 7.4, 140 mM NaCl, 10 mM CHAPS, 10% glycerol, 2 mM EDTA, Complete EDTA-free protease inhibitor mixture (Roche Applied Science)) and subjected to immunoprecipitation using antibodies in concentrations of 5 μg/ml. After binding of precipitated material to protein-G-Sepharose, eluates were analyzed by SDS-PAGE and subsequent Western blotting. Proteins were detected using either a-A10cyt or a-A10pro antibodies (1:1000, respectively) and anti-rabbit horseradish peroxidase as secondary antibody (1:5000; Sigma). Bands were visualized by chemiluminescence.

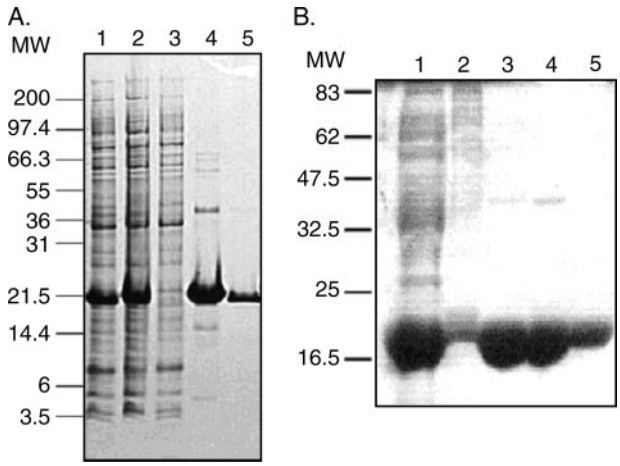

FIGURE 1. **SDS-polyacrylamide gel of ADAM10 prodomain wild type (23–213) and the C173S mutant.** *A,* prodomain of ADAM10 was obtained by lysis of bacteria and clarification by spinning at 20,000 rpm, then passing through Ni-NTA resin and eluting followed by a Superdex 75 sizing column. The molecular mass markers are in kDa. *Lane 1,* supernatant obtained after spinning lysis mixture at 20,000 rpm; *lane 2,* pellet obtained after lysis and spinning the supernatant to clarify; *lane 3,* flow through from Ni-NTA column; *lane 4,* eluted material from the Ni-NTA column; *lane 5,* sizing column fractions 11–17. *B,* C173S mutant was prepared as described above for the wild type prodomain. The molecular mass markers are in kDa. *Lane 1,* supernatant obtained after spinning lysis mixture at 22,500 rpm; *lane 2,* pellet obtained after lysis and spinning the supernatant to clarify; *lane 3,* eluted material from the Ni-NTA column; *lane 4,* sizing column fractions 11–16; *lane 5,* sizing column fractions 17–21.

RESULTS

Full-length Prodomain—Based on the work presented for the TACE prodomain (9), we prepared a construct encoding amino acids 23–213 of mouse ADAM10 prodomain. We constructed the 23–213 ADAM10 prodomain with either the N- or C-terminal His tag to ensure that the location of the His tag did not interfere with inhibition of ADAM10. Both of these constructs exclude the N-terminal hydrophobic signal sequence region and end at the furin cleavage site.

Initial induction tests of the ADAM10 prodomain at 37 °C showed that the expression level was low and that most of the protein was found in an insoluble pellet. By reducing the induction temperature from 37 to 20 °C, we were able to obtain milligram quantities of soluble ADAM10 prodomain after inducing for 16 h with 1 mM isopropyl β-D-thiogalactopyranoside. The prodomain was purified via a Ni^{2+}-NTA column followed by size-exclusion chromatography using a Superdex 75 column (Fig. 1*A*). The wild type prodomains 23–213, containing either the N- or C-terminal His tags, were both efficient inhibitors of ADAM10 (Table 1), with inhibition constants of 75 and 48 nM, respectively. We conclude that the ADAM10 prodomain inhibition does not depend on the location of the His tag.

Cysteine Switch Hypothesis—For metalloproteinases that exist as zymogens, the presence of a cysteine in their prodomains is often necessary for inhibition of catalytic activity. The cysteine is proposed to chelate the active site zinc ion of the metalloproteinase, causing the enzyme to remain in an inactive state. For some of the ADAM family members, the cysteine is required for efficient inhibition of the enzyme. We tested

TABLE 1

Inhibitory properties of ADAM10 prodomain 23–213

Enzyme was incubated with prodomain, and reaction progress was monitored with fluorescent substrates as described under "Experimental Procedures."

Inhibitor	Catalytic/disintegrin human ADAM10	Catalytic/disintegrin human TACE	Catalytic human TACE	Catalytic murine ADAM8	Catalytic/disintegrin human ADAM9	MMP-1–3, -9, -13, -14
Pro-A10 WT 23–213 (N-terminal His tag)	75 ± 15 nM	>3 μM	>11 μM	ND[a]	ND	>2 μM
Pro-A10 WT 23–213 (C-terminal His tag)[b]	48 ± 36 nM	>10 μM	>11 μM	50% at 10 μM	45% at 1 μM	>2 μM
ProA10 C173S 23–213 (C-terminal His tag)	36 ± 9 nM	>3 μM	>3 μM	50% at 10 μM	>1 μM	>2 μM

[a] ND means not determined.
[b] The inhibition constant was calculated from the initial velocities plot *versus* substrate concentration at varying concentrations of prodomain (see "Experimental Procedures").

TABLE 2

Inhibition of ADAM activities by mouse prodomains of TACE and ADAM8

Enzyme was incubated with either the mouse prodomains of ADAM8 or TACE. Reaction progress was monitored with fluorescent substrates as described under "Experimental Procedures."

Inhibitor	Catalytic/disintegrin human TACE	Catalytic human TACE	Catalytic/disintegrin human ADAM10	Catalytic murine ADAM8
Pro-A17	>3.5 μM	37% at 3.5 μM	11% at 3.5 μM	17% at 1.7 μM
Pro-A8	13% at 3 μM	50% at 3 μM	25% at 3 μM	9% at 3 μM

whether the cysteine in the putative cysteine switch of the ADAM10 prodomain affected the potency of inhibition by preparing a C-terminal His tag construct with the only cysteine mutated to serine. In Fig. 1*B* is a Coomassie-stained gel representing the purified C173S prodomain 23–213.

We found that the C173S ADAM10 prodomain 23–213 represents a tight and specific inhibitor of human ADAM10 with an inhibition constant of 36 ± 9 nM (Table 1). Furthermore, mouse ADAM10 catalytic activity[4] is inhibited with a K_i of 17 ± 10 nM, supporting the hypothesis that there are no species differences that account for the potency of ADAM10 prodomain. These results indicate that the cysteine residue in the ADAM10 prodomain is not required for efficient inhibition of catalytic activity, and the inhibitory mechanism of ADAM10 prodomain is distinct from the cysteine switch mechanism.

ADAM10 Prodomain as a Specific Inhibitor—Inhibition studies against ADAM and MMP family members were performed to evaluate the specificity of the ADAM10 prodomain. The inhibition was specific to ADAM10. The closely related family members, matrix metalloproteinases 1, 2, 3, 9, 13, and 14, were not inhibited by 3 μM cysteine containing C-terminal His tag wild type or C173S (residues 23–213) prodomains (Table 1). In addition, TACE catalytic and TACE catalytic/disintegrin enzymes were inhibited only slightly by the prodomains at concentrations of ~30 μM. Inhibition of ADAM8 was seen between 4 and 9 μM, and ADAM9 was inhibited with a K_i near 1 μM.

The potent inhibition of ADAM10 by its prodomain seems to be unique as the prodomains of TACE and ADAM8 only slightly inhibited their respective enzymes at micromolar concentrations (Table 2). The ADAM8 prodomain inhibited both TACE and ADAM10, but only at high concentrations.

ADAM10 Prodomain Exists as a Dimer in Solution—The retention time of a given protein on a gel filtration column often reflects its oligomeric state. The prodomain of ADAM10 consisting of residues 23–213 and both the wild type and the C173S mutant appeared to migrate on the Superdex-75 size-exclusion column as a dimer. We performed ultra-analytical centrifugation to determine the oligomeric state of the protein at various protein concentrations to confirm this observation. Fig. 2*A* shows the nonlinear least squares fit of the curve generated by sedimentation equilibrium. The molecular mass of the ADAM10 prodomain was in the range of 41.5 ± 1.3 kDa at the concentrations of 0.9 mg/ml as compared with a known monomer molecular mass of 23 kDa. The molecular weight did not vary at concentrations ranging from 0.45 to 1.8 mg/ml. The findings were comparable for both the Cys to Ser mutant and wild type protein. This suggests that ADAM10 prodomain exists in solution primarily as a dimer under these conditions.

Secondary Structure—We collected CD wavelength spectrum of the ADAM10 prodomain to gain information of the secondary structure of the ADAM10 prodomain and to confirm that this protein construct is folded. α-Helix, β-sheet, and random coil structures give rise to characteristic CD spectra. Typical α-helical proteins produce minima at 222 and 208 nm, whereas β-sheets exhibit minima at 215 nm. The CD spectrum (as shown in Fig. 2*B*) exhibits signals containing a mixture of α-helix and β-strand secondary structure and confirms that this construct is folded. The minimum at 222 nm largely suggests helical secondary structure content. However, the lack of a pronounced minimum at 208 nm indicates that a portion of this domain adopts a β-strand conformation.

Mechanism of Inhibition—The prodomain was tested to determine the mode of inhibition of ADAM10. Interestingly, a typical Lineweaver Burke plot, where the substrate was varied as a function of inhibitor concentration, gave curved lines for the reciprocal plot. Therefore, a $1/v$ *versus* $1/[S^2]$ plot was used and gave a good fit with the slopes varying but the intercepts remaining the same (Fig. 3). This indicated that the prodomain of ADAM10 is a competitive inhibitor of ADAM10 catalytic and disintegrin domain. The analysis also indicated that ADAM10 has at least two binding sites for the fluorescent substrate. The velocities *versus* substrate at varying inhibitor values were fit as a family of curves to the pure competitive inhibitor model. This gave the best fit from a selection of over seven other

[4] M. Moss, unpublished observations.

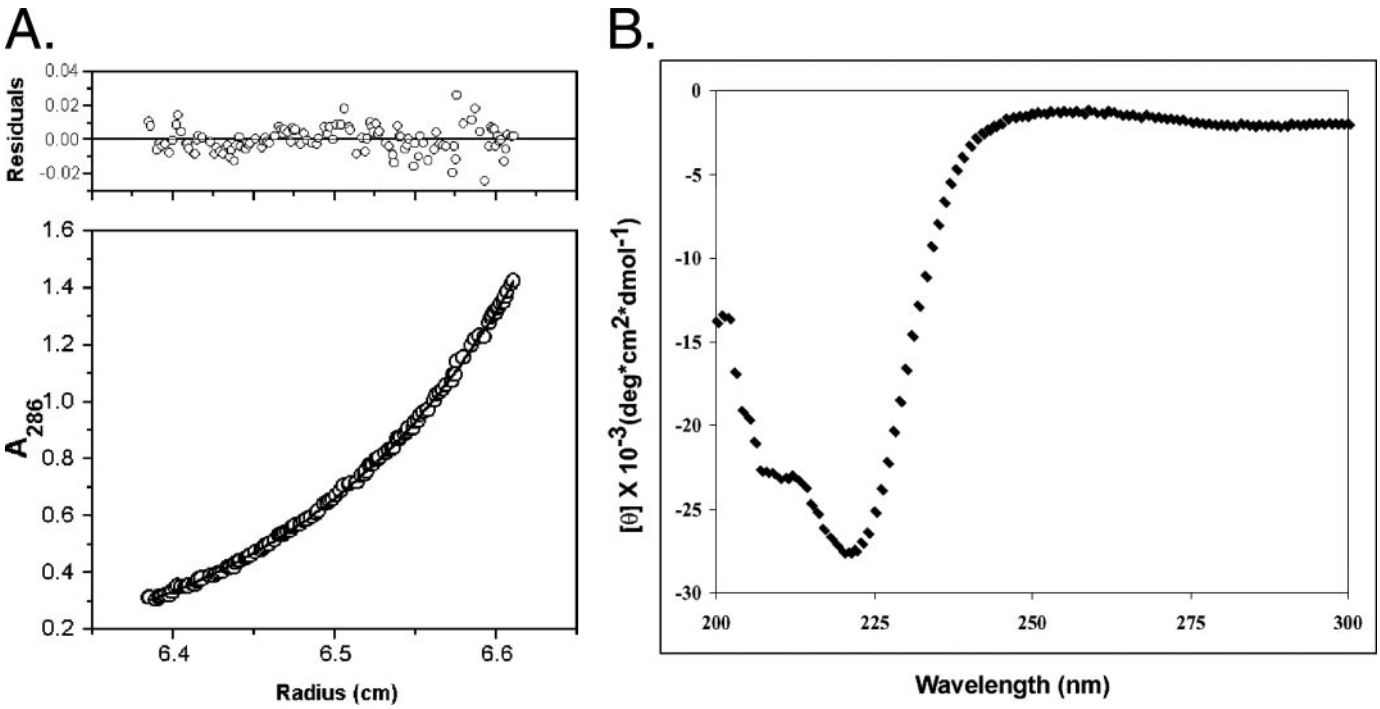

FIGURE 2. **Ultra-analytical centrifugation and CD spectrum of ADAM10 prodomain C173S mutation.** *A,* pattern shown is for a 0.9 mg/ml solution run at 15,000 rpm and at 25 °C. The best fit molecular weight was 40,400. *B,* CD spectrum of a 30 μM sample of ADAM10 prodomain from 200 to 300 nm indicating that this construct is folded, and a mixture of α-helices and β-sheets.

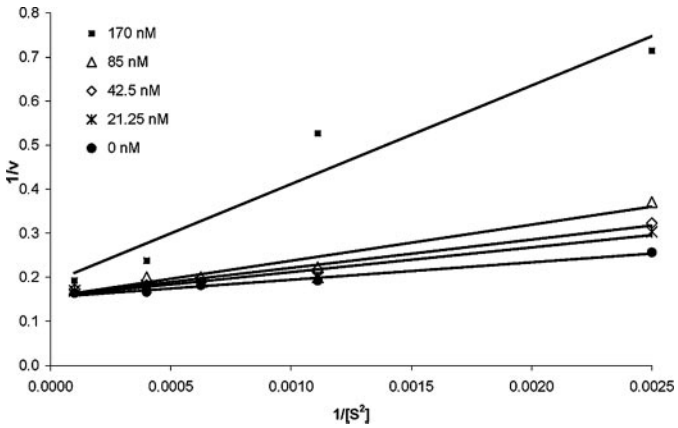

FIGURE 3. **Lineweaver Burke plot of 1/*v versus* 1/[S^2].** Initial velocities were obtained from the slopes of plots of fluorescence *versus* time graphs and plotted as a reciprocal *versus* a reciprocal of substrate concentration to the second power. The lines at varying inhibitor concentrations are intersecting at a common intercept, indicating that the prodomain of ADAM10 binds as a competitive inhibitor.

allosteric two-site models. The K_i, calculated with this method, was 48 ± 36 nM and the binding constant, K_s, for substrate was 16 ± 4.6 μM.

Truncation of the ADAM10 Prodomain—The prodomains, 23–213 and 23–213 Cys to Ser, were truncated to determine the minimal domain requirements for inhibition of ADAM10. Analysis of the secondary structure indicated that the prodomain could most likely be truncated at the C terminus without significantly disturbing its activity. Furthermore, limited proteolysis with trypsin and analysis of the processed prodomain via mass spectroscopy suggested that the prodomain could be modified at the C terminus. We prepared wild type constructs 23–176 and 23–181 and measured inhibition of ADAM10

TABLE 3
Inhibition of ADAM10 by truncated prodomains of ADAM10

Enzyme was incubated with truncated prodomains, and the fractional inhibition *versus* inhibitor concentration was plotted and fit to a hyperbolic function using the program Sigma Plot from Systat.

Inhibitor	Catalytic/disintegrin ADAM10
WT 23–176 (C-terminal His tag)	900 ± 454 nM
WT 23–181 (C-terminal His tag)	473 ± 174 nM
WT 18–176 (C-terminal His tag)	260 ± 35 nM
WT 18–176 (N-terminal His tag)	400 ± 92 nM
C173S 23–181 (C-terminal His tag)	>5 μM
C173S 23–181 (N-terminal His tag)	>5 μM

activity. The results are in Table 3. Both constructs were less potent inhibitors of ADAM10 with inhibition constants of 900 ± 45 and 473 ± 174, respectively. However, they still retained inhibitory activity. Addition of amino acids to the N terminus by five to generate 18–176 N- or C-terminal His (Table 3) did not seem to dramatically affect function, suggesting that these residues are not critical for prodomain binding to ADAM10. Further modification of the N terminus resulted in a prodomain that was expressed as an insoluble pellet in *E. coli*, and these constructs were not analyzed further. The Cys to Ser mutant was also shortened to amino acids 23–181. Interestingly, this mutant lost its inhibitory activity against ADAM10 and had an estimated inhibition constant of greater than 5 μM (Table 3). This truncated mutant also exists as a dimer in solution ruling out the possibility that inhibition of ADAM10 correlates with the ability of prodomain to aggregate.

Cell-based Assay with ADAM10 Prodomain—Previously, the effect of constitutive overexpression of the ADAM10 prodomain on APPsα shedding from HEK293 cells had been investigated (25). It has been proposed that the intracellular overexpression of the ADAM10 prodomain reduces APPsα shedding most likely by

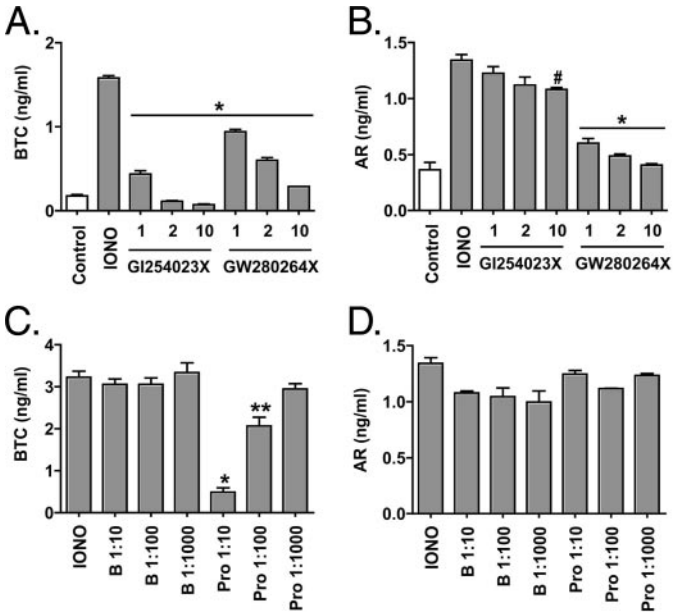

FIGURE 4. **Calcium ionophore-induced betacellulin shedding in IMPE cells is inhibited by ADAM10 prodomain.** Calcium ionophore-induced human BTC (*A* and *C*) and human AR (*B* and *D*) shedding in conditionally immortalized pancreatic epithelial (*IMPE*) cell lines was determined in the presence or absence of a selective ADAM10 inhibitor, GI254023X (1, 2, and 10 μM), a more broad spectrum metalloprotease inhibitor, GW280264X (1, 2, and 10 μM) (*A* and *B*), or with different concentrations of either the ADAM10 prodomain (1:10, 15 μM, and 1:100, 1.5 μM) or control buffer (1:10 and 1:100) by enzyme-linked immunosorbent assay measurements of conditioned media (*C* and *D*). BTC and AR shedding are expressed as soluble ligand shed into the conditioned media. *A*, ionophore (*IONO*) *versus* GI254023X (1, 2, or 10 μM) or GW280264X (1, 2, or 10 μM); * = $p < 0.001$. *B*, ionophore *versus* GI254023X (10 μM); $p < 0.05$; ionophore *versus* GW280264X (1, 2, or 10 μM), $p < 0.001$. *C*, ionophore *versus* prodomain 1:10, $p < 0.001$; ionophore *versus* prodomain 1:100, $p < 0.01$. Control and calcium ionophore-treated samples are represented by *white* and *gray bars*, respectively, and buffer alone and ADAM10 prodomain-treated samples are labeled as *B* or *Pro*, respectively.

interaction with mature ADAM10 either in the secretory pathway or at the cell surface (24). To determine whether adding back the ADAM10 prodomain could specifically inhibit the shedding of ADAM10 substrates, we tested the effects of exogenous, recombinant ADAM10 prodomain on the shedding of two ErbB ligands, BTC and AR, in cell-based cleavage assays. ADAM10 is responsible for constitutive and ionophore-induced shedding of betacellulin (11, 23), whereas ADAM17/TACE is responsible for constitutive and phorbol ester-induced amphiregulin shedding. Interestingly, ionophore-induced amphiregulin shedding is independent of ADAM10 but may only be partially dependent on ADAM17 (26).[5]

Because BTC shedding is activated by calcium ionophore treatment and not by phorbol ester treatment (23), we initially decided to examine the effect of the ADAM10 prodomain on calcium ionophore-induced shedding of BTC and AR in IMPE cells. To first demonstrate that ionophore-induced BTC and AR shedding in IMPE cells displays different metalloprotease specificities, we determined the effect of two metalloprotease inhibitors GI254023X (a selective ADAM10 inhibitor) and GW280264X (a more broad spectrum inhibitor) on these shedding events (27–29). Calcium ionophore treatment robustly stimulated both BTC and AR shedding in IMPE cells (Fig. 4, *A* and *B*). Importantly, calcium ionophore-induced BTC shedding was efficiently blocked in a dose-dependent manner by the ADAM10-specific inhibitor GI254023X (Fig. 4*A*), whereas GI254023X treatment had only minimal inhibitory effect on AR ionophore-induced shedding even at the highest dose in IMPE cells (Fig. 4*B*). These data are in agreement with our previous findings that calcium ionophore-induced BTC shedding is dependent on ADAM10 (23).

We next examined whether treatment with the ADAM10 prodomain could specifically block ionophore-induced BTC shedding in IMPE cells. As expected, the prodomain of ADAM10 was able to inhibit calcium ionophore-induced betacellulin release (Fig. 4*C*) in a dose-response fashion with 75% inhibition at 15 μM and 33% inhibition at 1.5 μM. Further analysis showed that the ADAM10 prodomain was also able to block constitutive and ionophore-induced BTC shedding in HEK293 and Madin-Darby canine kidney cells overexpressing human BTC (data not shown). The truncated ADAM10 prodomain 23–181, C173S mutant, that does not inhibit ADAM10 efficiently, had no effect on betacellulin shedding, indicating that inhibition of ADAM10 activity depends on the inhibitory properties of the prodomain.

Further proof that the prodomain specifically inhibits ADAM10 was obtained with cell-based assays used to assess amphiregulin shedding. No inhibition of calcium ionophore-induced AR shedding in IMPE cells was observed upon treatment with the ADAM10 prodomain (Fig. 4*D*). Moreover, the ADAM10 prodomain had no effect on other constitutive and phorbol ester-stimulated AR shedding events (data not shown). Together, these findings indicate that treatment with exogenous, recombinant ADAM10 prodomain can selectively inhibit the shedding of an ADAM10 substrate, betacellulin, through access to the shedding machinery from the cell surface.

Cellular Localization and Co-immunoprecipitation of Prodomain and Full-length ADAM10—As demonstrated above, the ADAM10 prodomain works as an inhibitor in cell-based assays. To address whether there is any evidence for an *in vivo* function of the prodomain, *e.g.* by regulating ADAM10 activity, we performed immunofluorescence in conjunction with immunoprecipitation by using two characterized antibodies against the prodomain and the cytoplasmic domain of ADAM10, respectively. The cDNA encoding full-length mouse ADAM10 was transiently transfected into COS1 cells. Cells were stained with antibodies either directed against the prodomain (a-A10pro) or the cytoplasmic tail (a-A10cyt) of ADAM10 in Triton X-100-permeabilized cells (Fig. 5, *A–M*). The antibody a-A10pro recognizes pro-ADAM10 and the released ADAM10 prodomain (Fig. 5, *B, E, H,* and *L*). Mostly, the prodomain signal, either covalently or noncovalently attached, is localized to intracellular vesicles within the cell, consistent with the observation that most of the protein is found in transport vesicles during passage through the trans-Golgi network; only a minor proportion of prodomain can be found close to the cell membrane. Consequently, staining with a-A10cyt shows a nearly identical distribution of ADAM10 in the cells analyzed. This finding demonstrates that active and inactive ADAM10 are indistinguishable in their cellular localizations, assuming that even active ADAM10 is co-localized with its prodomain under physiolog-

[5] P. Dempsey, personal observations.

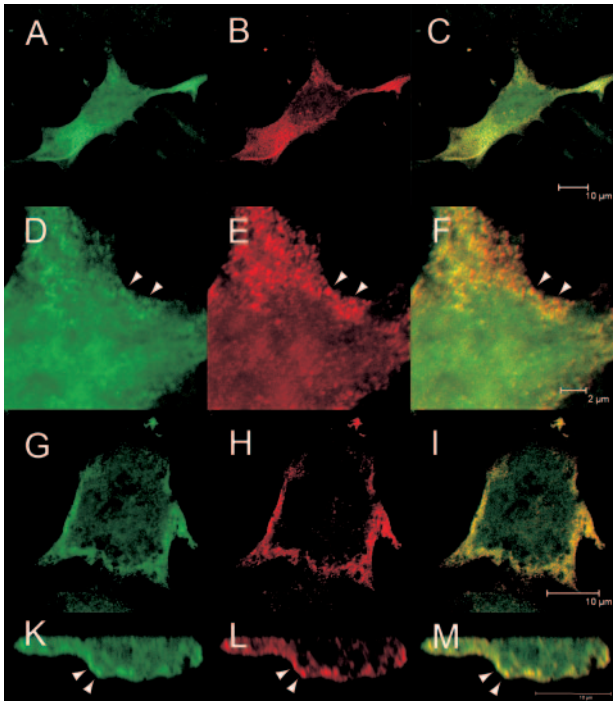

FIGURE 5. **Immunolocalization of ADAM10 prodomain and cytoplasmic domain in COS-1 cells.** COS-1 cells were transfected with an ADAM10 expression construct. After fixation and permeabilization with 0.1% Triton X-100, polyclonal antibodies were used either directed against the cytoplasmic domain (a-A10cyt, *green*) or the prodomain (a-A10pro, *red*) of ADAM10. The antibody a-A10cyt detects latent and processed ADAM10 (*A, D, G,* and *K*), whereas a-A10pro detects pro-ADAM10 and the cleaved prodomain (*B, E, H,* and *L*). *D–F*, detailed images of the cell shown in *A–C*. Note that ADAM10 is mainly localized to small vesicles during passage through the trans-Golgi network; some of those are depicted by *arrowheads* in *D–F* and *K–M*. In *C* and *F*, the signals obtained for both antibodies are overlapping, arguing for a co-existence of pro-ADAM10 with processed ADAM10 and the released ADAM10 prodomain. *K–M,* optical *xz* cross-section of a flattened cell shown in *G–I*, demonstrating the presence of the ADAM10-positive vesicles close to the cell membrane. No signals with either antibody were observed in nonpermeabilized cells. Note that *bar* in *C*, 10 μm, valid for *A–C*; *bar* in *F*, 2 μm, valid for *D–F*; *bar* in *I*, 10 μm, valid for *G–I*; *bar* in *M*, 10 μm, valid for *K–M*.

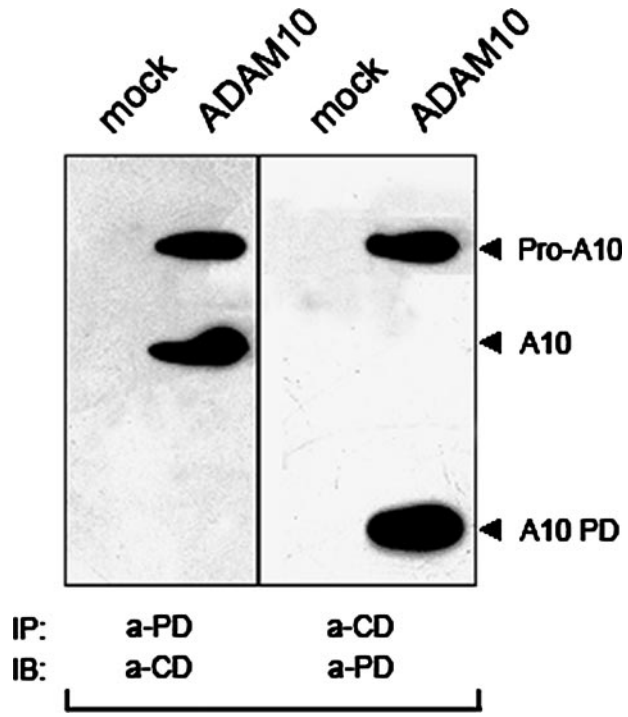

FIGURE 6. **Immunoprecipitation of ADAM10 prodomain from mock or ADAM10 transfected COS1 cells.** COS1 cell lysates were immunoprecipitated either with a-A10pro (*a-PD*) or a-A10cyt (*a-CD*) as indicated below (immunoprecipitation, antibodies used for immunoprecipitation). After protein-G-Sepharose isolation and PAGE, the blots were probed either with a-A10pro or a-A10cyt, as indicated (IB, antibodies used for immunoblotting). *Arrowheads* (*right*) indicate the positions on the blots for pro-ADAM10, mature ADAM10, and the ADAM10 prodomain.

ical conditions. In nonpermeabilized cells, *e.g.* without Triton X-100 treatment, no signals were obtained either with a-A10cyt or with a-A10pro (data not shown). The latter result confirms that no prodomain is found on the cell surface. These findings also argue for a tight intracellular regulation of ADAM10 activity by the persistent presence of the prodomain during ADAM10 maturation.

To support this hypothesis, immunoprecipitation experiments were performed using a-A10pro and a-A10cyt antibodies (Fig. 6). With a-A10pro antibodies, we were able to pull down pro-ADAM10 and processed ADAM10 in equal amounts (Fig. 6, *left panel*), ruling out the hypothesis that dimerization of prodomain is the reason why the prodomain is found in immunoprecipitates. Consequently, immunoprecipitation with a-A10cyt led to a pulldown of pro-ADAM10 and the ADAM10 prodomain. The finding that prodomain and mature ADAM10 are isolated in immunoprecipitates also demonstrates that at least some of the prodomain found co-staining with ADAM10 within the cell via immunofluorescence is no longer covalently attached to ADAM10. These findings collectively suggest that prodomain associates with mature ADAM10 within the cell.

DISCUSSION

We have provided evidence that the prodomain of mouse ADAM10 is a specific inhibitor of human ADAM10 activity both *in vitro* and in cell-based assays. To our knowledge, this is the first report of a specific inhibitor of ADAM10 (K_i = 48 nM) as other reported inhibitors, such as GI254023 and tissue inhibitors of metalloproteinases, inhibit MMPs as well as other ADAM family members. For example, the ADAM10 prodomain does not inhibit the activities of other ADAM proteases (8, 9, and 17) under conditions where full inhibition of ADAM10 is observed. Thus, the prodomain can be used in cellular assays to assess ADAM10 functions.

Interestingly, the prodomains truncated at the C terminus retain inhibitory activity although they are ~10-fold less potent than the full-length protein. Most of the inhibitory potential resides in a 40-amino acid region containing Cys-173 to Lys-213. In addition, the cysteine residue at position 173 is critical for inhibition in the truncated prodomain.

The prodomain also exists as a dimer, regardless of whether it is truncated at the C terminus to remove 32 amino acids. The cysteine (Cys-173) is also not required for dimerization. Fig. 6 implies that the stoichiometric ratio between prodomain and metalloproteinase domain is 2:1, and we tried to solve this question *in vitro*. However, we could not use the antibody setup we used for the *in vivo* immunoprecipitation, as the recombinant ADAM10 enzyme lacks the C-terminal domain (a-CD is generated against the peptide at amino acid position 727–741), whereas the recombinant ADAM10 is truncated at position

674. Moreover, Western analysis after a pulldown using Ni-NTA resin is not feasible as both the recombinant ADAM10 and the prodomain contain His tags. Under this experimental setup, the only way to determine the stoichiometry would be ultra-analytical centrifugation or titration experiments, but this is impracticle because of limited quantities of the ADAM10 protein from a commercial source. The mouse ADAM10 prodomain is also unique in its ability to inhibit potently the ADAM10 catalytic/disintegrin domain. In contrast, the mouse prodomain of TACE only modestly inhibits the activities of human TACE catalytic domain and human ADAM10 catalytic/disintegrin domain, respectively (9). In addition, no effect on activity is seen for micromolar concentrations of the prodomain for the human TACE catalytic/disintegrin domain construct. Mouse ADAM8 prodomain only slightly inhibits mouse ADAM8 catalytic domain, and does not inhibit the human ADAM8 catalytic/disintegrin domain.[4] However, it does suppress human TACE and ADAM10 activities. Because other ADAM family members do not seem to bind tightly to their respective prodomains even in an *in vitro* assay, it is unlikely for other members to directly associate with mature ADAMs *in vivo*.

The ability of prodomains to inhibit enzymes does not seem to rely on overall identity with each other. Mouse ADAM10 prodomain has the most identity to human ADAM10 prodomain (92%) followed by human TACE prodomain (28% over a 126-amino acid stretch). This could explain why TACE prodomain inhibits to some extent ADAM10. There is very little identity except when comparing one prodomain among different species. A noteworthy observation is that the cysteine switch region of mouse ADAM8 prodomain shares 40% identity with TACE prodomain. This finding could explain why mouse ADAM8 prodomain inhibits both TACE constructs.

ADAM10 prodomain co-localizes with ADAM10 within the cell in vesicles. In addition, the prodomain co-immunoprecipitates with mature and full-length ADAM10 when transfected into COS-1 cells. Co-precipitation of prodomain with ADAM10 could occur through intermediary proteins. However, our findings demonstrate that prodomain associates directly *in vitro* with ADAM10 with a nanomolar inhibition constant. Therefore, collectively, these experiments confirm that the ADAM10 prodomain is likely to be associated with ADAM10 *in vivo* either before or after the pro-ADAM10 has undergone processing by a proprotein convertase.

The specificity and potency of the ADAM10 prodomain make it a good candidate for ADAM10 antagonist activity *in vivo*. In a betacellulin assay, the prodomain was an inhibitor. Because the K_i value in our activity assays lies within the nanomolar range, it is unclear why micromolar quantities of prodomain are required in this assay. Precedence for this comes from inhibitors of ADAM10 used in this study. Often micromolar quantities of inhibitor are required in cell-based assays that measure release of proteins even though the same inhibitors are nanomolar against the enzyme in an *in vitro* assay. GM6001 is an example of this as its IC_{50} is 1.7 nM against TACE in an enzyme assay but is micromolar in cell-based shedding assays. We have found that GI254023X inhibits ADAM10 in the nanomolar range but has an IC_{50} of micromolar range for betacellulin release. In addition, tissue inhibitors of metalloproteinases are required in micromolar quantities in shedding assays even though they are subnanomolar physiological inhibitors of MMPs and ADAMs (30). These findings indicate that the prodomain of ADAM10 may be able to inhibit ADAM10 *in vivo* even though micromolar quantities are used in shedding assays.

An alternative hypothesis, although unlikely, is that ADAMs other than ADAM10 are involved in processing of ErbB ligands. ADAM9, for example, possesses EGF processing activity (31), and other as yet undiscovered ADAMs may cleave betacellulin. It will be interesting to analyze what other biological processes are dependent on ADAM10. The high expression level and stability of the prodomain in cell-based assays makes it well suited for further structural and functional studies.

Acknowledgments—We thank Dr. Marcos Milla (University of Pennsylvania) for providing the TACE catalytic domain and helpful comments and Edward Crutcher for technical assistance.

REFERENCES

1. Moss, M. L., and Bartsch, J. W. (2004) *Biochemistry* **43,** 7227–7235
2. Blobel, C. P. (2005) *Nat. Rev. Mol. Cell Biol.* **6,** 32–43
3. Black, R. A., Doedens, J. R., Mahimkar, R., Johnson, R., Guo, L., Wallace, A., Virca, D., Eisenman, J., Slack, J., Castner, B., Sunnarborg, S. W., Lee, D. C., Cowling, R., Jin, G., Charrier, K., Peschon, J. J., and Paxton, R. (2003) *Biochem. Soc. Symp.* **70,** 39–52
4. Blobel, C. P., Wolfsberg, T. G., Turck, C. W., Myles, D. G., Primakoff, P., and White, J. M. (1992) *Nature* **356,** 248–252
5. Milla, M. E., Leesnitzer, M. A., Moss, M. L., Clay, W. C., Carter, H. L., Miller, A. B., Su, J. L., Lambert, M. H., Willard, D. H., Sheeley, D. M., Kost, T. A., Burkhart, W., Moyer, M., Blackburn, R. K., Pahel, G. L., Mitchell, J. L., Hoffman, C. R., and Becherer, J. D. (1999) *J. Biol. Chem.* **274,** 30563–30570
6. Hougaard, S., Loechel, F., Xu, X., Tajima, R., Albrechtsen, R., and Wewer, U. M. (2000) *Biochem. Biophys. Res. Commun.* **275,** 261–267
7. Loechel, F., Overgaard, M. T., Oxvig, C., Albrechtsen, R., and Wewer, U. M. (1999) *J. Biol. Chem.* **274,** 13427–13433
8. Fahrenholz, F., Gilbert, S., Kojro, E., Lammich, S., and Postina, R. (2000) *Ann. N. Y. Acad. Sci.* **920,** 215–222
9. Gonzales, P. E., Solomon, A., Miller, A. B., Leesnitzer, M. A., Sagi, I., and Milla, M. E. (2004) *J. Biol. Chem.* **279,** 31638–31645
10. Van Wart, H. E., and Birkedal-Hansen, H. (1990) *Proc. Natl. Acad. Sci. U. S. A.* **87,** 5578–5582
11. Sahin, U., Weskamp, G., Kelly, K., Zhou, H. M., Higashiyama, S., Peschon, J., Hartmann, D., Saftig, P., and Blobel, C. P. (2004) *J. Cell Biol.* **164,** 769–779
12. Pan, D., and Rubin, G. M. (1997) *Cell* **90,** 271–280
13. Lammich, S., Kojro, E., Postina, R., Gilbert, S., Pfeiffer, R., Jasionowski, M., Haass, C., and Fahrenholz, F. (1999) *Proc. Natl. Acad. Sci. U. S. A.* **96,** 3922–3927
14. Kojro, E., and Fahrenholz, F. (2005) *Subcell. Biochem.* **38,** 105–127
15. Postina, R., Schroeder, A., Dewachter, I., Bohl, J., Schmitt, U., Kojro, E., Prinzen, C., Endres, K., Hiemke, C., Blessing, M., Flamez, P., Dequenne, A., Godaux, E., van Leuven, F., and Fahrenholz, F. (2004) *J. Clin. Investig.* **113,** 1456–1464
16. Huovila, A. P., Turner, A. J., Pelto-Huikko, M., Karkkainen, I., and Ortiz, R. M. (2005) *Trends Biochem. Sci.* **30,** 413–422
17. Zhou, B. B., Fridman, J. S., Liu, X., Friedman, S. M., Newton, R. C., and Scherle, P. A. (2005) *Exp. Opin. Investig. Drugs* **14,** 591–606
18. Moss, M. L., and Rasmussen, F. H. (2007) *Anal. Biochem.* **366,** 144–148
19. Rasmussen, F. H., Yeung, N., Kiefer, L., Murphy, G., Lopez-Otin, C., Vitek, M. P., and Moss, M. L. (2004) *Biochemistry* **43,** 2987–2995
20. Naus, S., Reipschlager, S., Wildeboer, D., Lichtenthaler, S. F., Mitterreiter, S., Guan, Z., Moss, M. L., and Bartsch, J. W. (2006) *Biol. Chem.* **387,** 337–346

21. Moss, M. L., and Lambert, M. H. (2002) *Essays Biochem.* **38,** 141–153
22. Koizumi, M. D. R., Mori, T., Kami, K., Ito, D., Tulachan, S., Toyoda, E., Masui, T., Kawaguchi, M. N. S., Tsuiji, S., Whitehead, R. H., Fujimoto, K., and Imamura, M. (2002) *Gastroenterology* **122,** Suppl. 1, 245–246
23. Sanderson, M. P., Erickson, S. N., Gough, P. J., Garton, K. J., Wille, P. T., Raines, E. W., Dunbar, A. J., and Dempsey, P. J. (2005) *J. Biol. Chem.* **280,** 1826–1837
24. Seed, B., and Aruffo, A. (1987) *Proc. Natl. Acad. Sci. U. S. A.* **84,** 3365–3369
25. Anders, A., Gilbert, S., Garten, W., Postina, R., and Fahrenholz, F. (2001) *FASEB J.* **15,** 1837–1839
26. Horiuchi, K., Le Gall, S., Schulte, M., Yamaguchi, T., Reiss, K., Murphy, G., Toyama, Y., Hartmann, D., Saftig, P., and Blobel, C. P. (2007) *Mol. Biol. Cell* **18,** 176–188
27. Hundhausen, C., Misztela, D., Berkhout, T. A., Broadway, N., Saftig, P., Reiss, K., Hartmann, D., Fahrenholz, F., Postina, R., Matthews, V., Kallen, K. J., Rose-John, S., and Ludwig, A. (2003) *Blood* **102,** 1186–1195
28. Budagian, V., Bulanova, E., Orinska, Z., Ludwig, A., Rose-John, S., Saftig, P., Borden, E. C., and Bulfone-Paus, S. (2004) *J. Biol. Chem.* **279,** 40368–40375
29. Ludwig, A., Hundhausen, C., Lambert, M. H., Broadway, N., Andrews, R. C., Bickett, D. M., Leesnitzer, M. A., and Becherer, J. D. (2005) *Comb. Chem. High Throughput Screen* **8,** 161–171
30. Wei, S., Kashiwagi, M., Kota, S., Xie, Z., Nagase, H., and Brew, K. (2005) *J. Biol. Chem.* **280,** 32877–32882
31. Peduto, L., Reuter, V. E., Shaffer, D. R., Scher, H. I., and Blobel, C. P. (2005) *Cancer Res.* **65,** 9312–9319